RSC Advances

PAPER

View Article Online
View Journal | View Issue

Cite this: *RSC Adv.*, 2024, **14**, 6617

Stereochemical insights into β-amino-*N*-acylhydrazones and their impact on DPP-4 inhibition†

Eduardo Reina,[a] Lucas Silva Franco,[ab] Teiliane Rodrigues Carneiro,[a] Eliezer J. Barreiro[ab] and Lidia Moreira Lima*[ab]

Dipeptidyl peptidase IV (DPP-4) is a key enzyme that regulates several important biological processes and it is better known to be targeted by gliptins as a modern validated approach for the management of type 2 diabetes mellitus (T2DM). However, new generations of DPP-4 inhibitors capable of controlling inflammatory processes associated with chronic complications of T2DM are still needed. In this scenario, we report here the design by molecular modelling of new β-amino-*N*-acylhydrazones, their racemic synthesis, chiral resolution, determination of physicochemical properties and their DPP4 inhibitory potency. Theoretical and experimental approaches allowed us to propose a preliminary SAR, as well as to identify LASSBio-2124 (**6**) as a new lead for DPP-4 inhibition, with good physicochemical properties, favourable eudismic ratio, scalable synthesis and anti-diabetes effect in a proof-of-concept model. These findings represent an interesting starting point for the development of a new generation of DPP-4 inhibitors, useful in the treatment of T2DM and comorbidities.

Received 17th January 2024
Accepted 17th February 2024

DOI: 10.1039/d4ra00450g

rsc.li/rsc-advances

Introduction

Dipeptidyl peptidase-4 (DPP-IV/DPP-4/CD26, EC3.4.14.5) is a 766 amino acid serine protease belonging to the α,β-hydrolase (family S9B), sequentially related to the prolyl oligopeptidases (POPs). DPP-4 specifically cleaves X-proline (X-pro) or X-alanine (X-ala) dipeptides from the free N-terminal sequence of peptides.[1,2] Almost all peptides bearing an X-pro or X-ala sequence are potential substrates for DPP-4, including cytokines, chemokines, growth factors and several peptides such as pituitary adenylate cyclase-activating polypeptide, peptide YY, substance P, neuropeptide Y and glucagon-like peptide-1 (GLP-1).[2–4] DPP-4 mediates limited proteolysis of these peptides resulting in their activation, activity modulation or initiation of degradation process. Thus, it has been linked to the regulation of blood pressure, immune system, and glucose control.[3,4]

In diabetes, DPP-4 is of particular importance as it is the enzyme involved in the GLP-1 metabolism. After secretion, GLP-1 is rapidly hydrolysed and inactivated by DPP-4 action (GLP-1 half-life = 2–4 minutes), making its use as a natural antidiabetic drug impossible.[3,4] Therefore, the development of DPP-4 inhibitors has emerged as a central strategy to circumvent this limitation and DPP-4 is a validated target to develop new drugs to treat type 2 diabetes mellitus (T2DM).[5] Although it is expected that DPP-4 inhibitors may prevent or delay the onset of chronic complications of diabetes, due to their ability to minimise the damage promoted by glucotoxicity process,[6] it should be considered that many patients that are diagnosed with T2DM already show significant damage to the macro- and microcirculation.[7] These damages, mainly due to local inflammation and oxidative stress, are not reversed or controlled by DPP-4 inhibitors.

In continuity with a line of research aimed at discovering new candidates for antidiabetic drugs, we conjecture the possibility of combining in a same molecule the structural features that confer the ability to inhibit DPP-4 and to modulate TNF-α production, a key player in the development of sub-chronic inflammation. This approach seeks to broaden the therapeutic spectrum of conventional DPP-4 inhibitors, enabling them to control the hyperglycaemia and to prevent or to regulate the chronic complications of diabetes.

Therefore, we proposed molecular hybridisation between and sitagliptin (Januvia®) (**1**), the first DDP-4 inhibitor approved by the FDA for the treatment of T2DM[8] and the prototype discovered by our group, LASSBio-1773 (**2**), which was described as a hypoglycemic agent able to reduce thermal hyperalgesia and mechanical allodynia in a murine model of STZ-induced diabetic neuropathic pain[9–11] (Fig. 1). In addition, LASSBio-1773 (**2**) has revealed important ability to modulate the

[a]*Instituto Nacional de Ciência e Tecnologia de Fármacos e Medicamentos (INCT-INOFAR), Laboratório de Avaliação e Síntese de Substâncias Bioativas (LASSBio®), Universidade Federal do Rio de Janeiro (UFRJ), CCS, Cidade Universitária, Rio de Janeiro-RJ, Brazil. E-mail: lidialima@ufrj.br*

[b]*Pós-graduação em Farmacologia e Química Medicinal, Instituto de Ciências Biomédicas, Universidade Federal do Rio de Janeiro, Rio de Janeiro-RJ, Brazil*

† Electronic supplementary information (ESI) available. See DOI: https://doi.org/10.1039/d4ra00450g

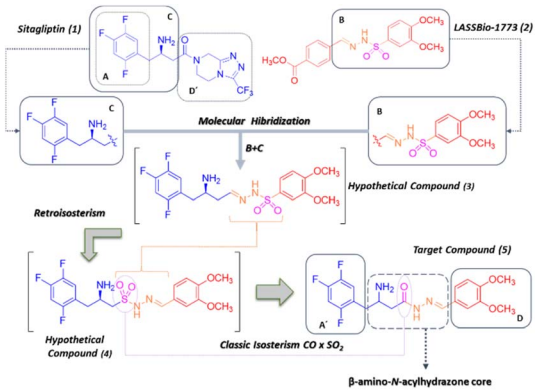

Fig. 1 Design concept of the new the β-amino-*N*-acylhydrazone derivative (**5**) proposed as a DPP-4 inhibitor by molecular hybridisation between sitagliptin (**1**) and LASSBio-1773 (**2**).

production of TNF-α, an important cytokine involved in sub-chronical and chronical inflammatory stages.[9–11]

Our conceptual design was guided by the need to retain the structural requirements described for enzyme inhibition,[5,8,12,13] such as: (1) a hydrophobic region (described for sitagliptin by subunit A, Fig. 1); (2) a primary or secondary amine group (which appears to be responsible for the selectivity towards prolyl endopeptidases, described for sitagliptin by subunit C, Fig. 1); and (3) a spacer or a linker connecting both the hydrophobic group and the amine group to a second aromatic subunit (D, Fig. 1), which has been proposed as the region of the molecule promoting selectivity over other exo-amino(di) peptidases.

One of the most notable features of the resulting hybrid compound (**5**) is the presence of the β-amino-*N*-acylhydrazone core (Fig. 1), which possess particular stereochemical properties in terms of absolute configuration and conformation (Fig. 2). With this assumption in mind, a key objective was to investigate the impact of selected five variables of the β-amino-*N*-acylhydrazone core, described in Fig. 2, on the DDP-4 enzymatic

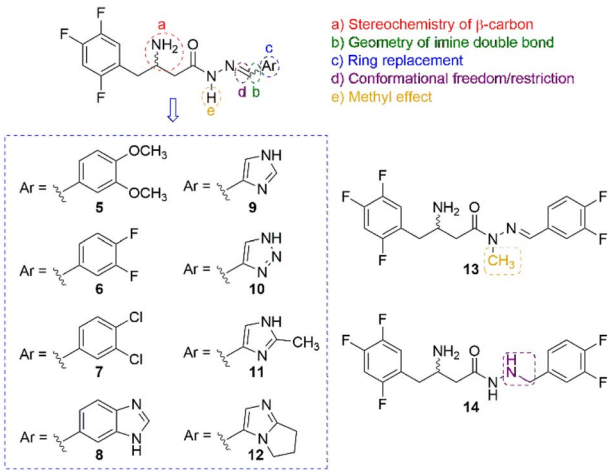

Fig. 2 Selected variables considered in the study of the β-amino-*N*-acylhydrazone core.

activity. We first carried out a molecular modelling study on DPP-4 enzyme to design the target compounds that represented the five variables under investigation (Fig. 2). Next, the designed compounds were synthesized and tested against DPP-4 enzyme *in vitro*. Our findings allowed us to propose a preliminary SAR model that may be useful in the design of new DPP-4 inhibitors with anti-inflammatory activity. In addition, our results suggest that the combination of the anti-inflammatory activity with inhibition of the DPP-4 enzyme could be explored to improve the current profile of DPP-4 inhibitors.

Taken together, these results are also important beyond their implications for T2DM therapies, considering that DPP-4 is a pharmacological target that remains of considerable ongoing interest, with several studies suggesting that DPP-4i could be used for other important indications such as cardiometabolic diseases,[14,15] atherosclerosis,[16] Alzheimer's disease[17–20] and viral pathologies, including COVID-19.[21,22]

Results and discussion

Design concept

The starting point of our design concept was the application of molecular hybridisation between the C-subunit of sitagliptin (**1**) and the B-subunit of LASSBio-1773 (**2**) (Fig. 1). Subsequently, the design of compound (**4**) was envisioned through the application of a retroisosterism strategy.[23] Considering several evidence of the isosteric relationship between sulfonylhydrazone ($RSO_2NHN{=}CHR$) and *N*-acylhydrazone ($RCONHN{=}CHR$) functions,[23,24] based primarily on the classical isosterism of carbonyl (CO) *versus* sulfonyl (SO_2) group, we designed compound (**5**) as the desired hybrid compound. It is noteworthy that the *N*-acylhydrazone framework has been reported as a privileged structure for the design of several bioactive compounds, including anti-inflammatory agents acting by different mechanism of action.[25] Thus, the proposed replacement of the SO_2 group by the CO group could potentially preserve the anti-inflammatory profile of the original prototype LASSBio-1773 (**2**). The structural analysis of the designed compound (**5**) allowed us to identify five variables, two related to the absolute configuration and three related to conformational changes, that may influence its theoretical degree of affinity by DPP-4. First, the stereochemistry nature of the carbon bearing the amine group, given that the eudysmic ratio for the two enantiomers of sitagliptin (**1**) is well known, with the *R*-enantiomer being the eutomer with an IC_{50} = 20 nM and the *S*-enantiomer being the distomer with IC_{50} = 440 nM.[26] Second, the geometry of the imine double bond since *E* or *Z* isomers will exhibit remarkably different orientations of the D-subunit in the pocket 2 of the DPP-4 enzyme (ESI Fig. S1†). Third, ring replacement of the D-subunit with other aromatic groups, which were designed as a congeneric series by replacing the 3,4-dimethoxyphenyl group in compound **4** (D-subunit, Fig. 2) with other related aromatic rings, resulting in compounds (**5–12**). Fourth, we decided to investigate the impact of increasing conformational freedom of the β-amino-*N*-acylhydrazone core on DDP-4 inhibition by designing compound (**13**) *via* reduction of the imine double bond. Finally, we designed compound (**14**)

by methylation of the sp^3 nitrogen of the β-amino-*N*-acylhydrazone core (Fig. 2) to evaluate the impact of the methylation effect in the NAH framework, a strategy that has been reviewed.[27] To evaluate these five variables, initially we first performed a molecular docking study of the designed compounds (Fig. 2) using a DPP-4 co-crystallized with sitagliptin (**1**), as follows.

Molecular modelling studies

Molecular docking studies of the newly designed compounds (**5–14**) were performed using the co-crystallographic structure of DPP-4 with sitagliptin (**1**), available in Protein Data Bank (PDB) with code 1 × 70.[26] All protein structures were obtained from human DPP-4 enzyme and showed a reasonable resolution (<2.85 Å). After validation by re-docking approach, the ChemPLP score function (without water) showed the best RMSD value (0.387 Å) (ESI Fig. S3†) and was therefore selected to perform the docking studies with the designed compounds (**5–14**).

β-Amino group stereochemistry. Compounds (**5–12**) in both configurations (*R* and *S*) were subjected to a docking study, keeping the geometry of the imine double bond fixed in the form of the *E* isomer. The scores obtained are summarized in Table 1, using GOLD 5.1 software. As expected from the eudysmic ratio described for sitagliptin (**1**), the docking study also identified differences in the *in silico* binding profile of the *S*- and *R*-enantiomers of sitagliptin (**1**) (ESI Fig. S4†). Regarding the *in silico* binding mode profile of the *S*- and *R*-enantiomers of compounds (**5–12**), the results generally showed that *R* stereoisomers had a better score value compared to the *S*-enantiomers, anticipating the eutomer profile of *R* isomers (Table 1). The compound bearing the 3,4-difluorophenyl subunit linked to the imine bond (*i.e.*, compound **6**) showed the best score value and a theoretical eudysmic profile very similar to that found for *R*-sitagliptin (**1-*R***) (Table 1). Compound (**6-*R***) was able to reproduce the orientation of sitagliptin in the active site of DPP-4 (Fig. 3), where the 2,4,5-trifluorophenyl moiety makes hydrophobic interactions in S1 the pocket, involving residues Val656, Trp659, Tyr666, Val711 and Tyr631; the primary amine makes ionic interactions with Glu205 and Glu206, besides the hydrogen bonding interaction with the side chain of Tyr662. Considering the introduction of the *N*-acylhydrazone, it is possible to visualise an additional hydrogen bonding interaction with the carbonyl group of the side chain of Glu206 and the amide hydrogen of compound (**6-*R***). On the other hand, the stereoisomer (**6-*S***) has shown a different orientation in the active site of DPP-4, with the D-subunit being orientated outside of the pocket S2. This change has resulted in the loss of the hydrogen bonding of the amide hydrogen with Glu206 and the π-stacking of 3,4-difluorophenyl with Phe357 (Fig. 3).

Table 1 Score values obtained with GOLD 5.1 for compounds **5–12** (*R*, *S*), using the ChemPLP score function

Compound	Score (*R*)	Score (*S*)
Sitagliptin (**1**)	88.02	72.01
(**5**)	83.9	75.1
(**6**)	86.9	79.3
(**7**)	84.6	82.3
(**8**)	80.2	77.1
(**9**)	79.7	70.2
(**10**)	74.2	67.9
(**11**)	76.4	71.2
(**12**)	80.3	75.8

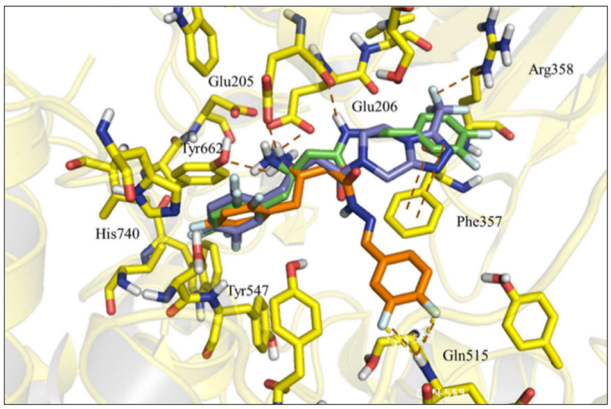

Fig. 3 Superposition of compounds (**6-*R***) (blue), (**6-*S***) (orange) and sitagliptin (**1-*R***) (green) inside DPP-4 active site.

Imine double bond geometry. We selected compound (**6-*R***) and studied the comparative binding mode for its *Z* and *E* geometric isomers. The stereochemistry of the imine double bond plays an important role in the molecular complementarity between the β-amino-*N*-acylhydrazones and the DPP-4 active site. While the (**6-*R***) *E* isomer has a binding mode and score (86.9) value close to that of (*R*)-sitagliptin (**1-*R***) (88.0), the (**6-*R***) *Z* isomer (76.3) shows a different orientation at the DPP-4 active site (Fig. 4) (ESI Table S2†). The remarkable change in orientation of the (**6-*R***) *Z* isomer is related to the 2,4,5-trifluorophenyl group in the (**6-*R*-*Z***)-isomer, which was positioned outside of the hydrophobic S1 pocket, and resulted in the loss of interactions performed by *R*-sitagliptin and the (**6-*R***)-*E* isomer. Taken together, these results indicate that the absolute configuration *R* and imine double bond relative configuration *E* are the most favourable for designing DPP-4 inhibitors.

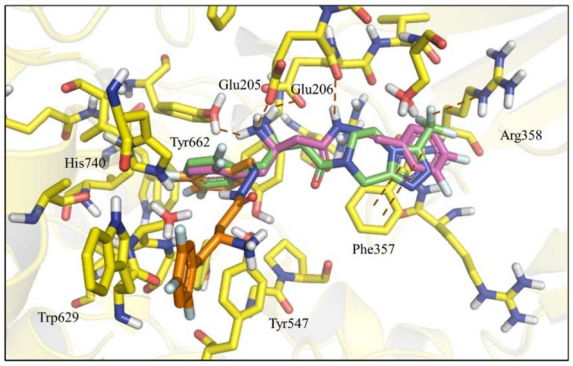

Fig. 4 Superposition of compounds (**6-*R*-*E***) (purple), (**6-*S*-*Z***) (orange) and *R*-sitagliptin (**1-*R***) (green) at the DPP-4 active site.

Conformational differences caused by D-subunit ring substitutions. Initially, we proposed eight types of modifications at the D-subunit (Fig. 2). For the *R*-enantiomers, with the imine double bond configuration fixed as the *E*-isomer, no significant differences were found either in the score values or in the ligand binding mode, when the aromatic group was a 3,4-dimethoxyphenyl (**5**) or a 3,4-dichlorophenyl (**5**) subunit.

Nevertheless, a higher score was found for compound (**6-*R***), which showed a similar binding mode to *R*-sitagliptin (**1-*R***). The attempt to replace the 3,4-dimethoxyphenyl by a benzimidazole or imidazole ring or by a pyrrolo[1,2-*a*]imidazole nucleus has resulted in a decrease in the score value, which was even more pronounced when 1,2,3-triazol or 2-methyl imidazole systems were docked (ESI Fig. S5†). With this information in mind, our next step was to study how conformational changes introduced directly into the β-amino-*N*-acylhydrazone framework would affect the binding to DPP-4. First, the increase in conformational freedom by reducing the β-amino-*N*-acylhydrazone core was investigated, and second, the impact of the methylation effect by substitution of the amidic hydrogen was investigated.[26]

Increased conformational freedom. According to the docking studies performed with compound (**13-*R***) (Fig. 5) (ESI Table S3†), the reduction of the imine double bond was expected to be favourable for the molecular recognition by DPP-4. Compound (**13-*R***) was able to maintain the ionic bridge with Glu205/Glu206. The 2,4,5-trifluorophenyl and 3,4-difluorophenyl moieties were predicted to perform different interactions with DPP-4. First, by exploring a hydrogen bond between the Trp629 and the fluorine atom of the 3,4-difluorphenyl subunit and a π-stacking interaction between the two aromatic rings. It is interesting to note that similar interactions have been reported for the quinazoline group of linagliptin[28] (ESI Fig. S6†). Secondly, a π-stacking interaction between Phe357 and the 2,4,5-trifluorophenyl ring. Finally, additional hydrogen interactions of the secondary amine hydrogens with Ser630 and Tyr547 were observed (Fig. 5).

Conformational changes induced by *N*-methylation of the β-amino-*N*-acylhydrazone core. The changes in *N*-acylhydrazone conformations due to methylation of the amide nitrogen have been previously acyl hydrazide.[27] As described by Barreiro and co-workers, LASSBio-294 has a typical linear conformation, whereas its *N*-methyl analogue (*i.e.*, LASSBio-785) has displayed a hairpin-like conformation (ESI Fig. S7†). These differences were also found between compounds (**6-*R***) and (**14-*R***) in the active binding of DPP-4 (ESI Fig. S8†). However, X-ray diffraction studies are still required to investigate such a conformational comparison.

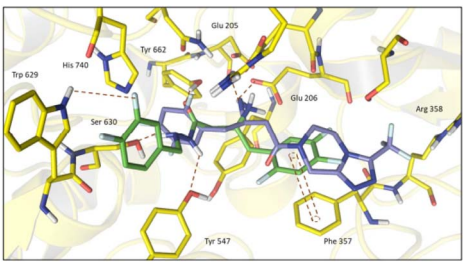

Fig. 5 Superposition of compounds (**13-*R***) (green) and *R*-sitagliptin (**1-*R***) (purple) inside DPP-4 active site.

Synthesis and structural characterization

To confirm the modelling results, we proposed to synthesise compounds that could represent each variable of interest (Fig. 2). In terms of the stereochemistry of the β-carbon atom linked to the amino group, we proposed to obtain (**6-*R***), its enantiomer (**6-*S***) and its racemate (**6-*R*,*S***). The geometry *Z* was predicted as detrimental in all the compounds analysed and, in addition, it has been established that obtaining of *Z* diastereoisomers NAH is thermodynamically unfavourable, so we expected and verified the *E*-geometry of all the β-amino-*N*-acylhydrazones synthesised. Regarding the third variable, the conformational changes promoted by the D-subunit substitution, it was observed two possible orientations, one that could be represented by the synthesis of (**6-*R***), and the second one, that could be represented by compounds (**5**) and (**7**), which have presented high scores and an adequate drug-like profile (ESI Table S4†). On the other hand, compound (**9**) was selected as a "negative control", as it was predicted to be a weak ligand to the DPP-4 binding site and to have unsatisfactory drug-like properties (ESI Table S4†). Finally, as previously discussed, the proposed change in the conformational nature of the β-amino-*N*-acylhydrazone framework by *N*-methylation and imine double bond reduction, was predicted to be favourable for compound (**14**) and unfavourable for compound (**13**). Therefore, both compounds were selected for synthesis and evaluation against DPP-4 enzyme.

To obtain the target compounds designed and selected by the docking studies two synthetic approaches were proposed. The first, exploring a synthetic route to obtain the target compounds as racemic mixtures, as depicted in Scheme 1A. The second approach was based on the synthesis of the enantiomerically pure compounds from the chiral resolution of the β-amino ester intermediate (**20**) (Scheme 1B).

The racemic synthesis of the selected compounds started with the synthesis of Meldrum's adduct (**17**), which was prepared by the reaction of 2,4,5-trifluorophenylacetic acid (**15**) with Meldrum acid (**16**) in the presence of CDI under inert atmosphere (Scheme 1).[29] Treatment of Meldrum's adduct (**17**) with MeOH under reflux in inert atmosphere yielded the β-keto ester (**18**), which was subjected to reductive amination in two steps. First, the β-enaminoester (**19**) was formed by treating the β-keto ester (**18**) with ammonium acetate in methanol under inert atmosphere (Scheme 1B). The β-enamine ester was then reduced with sodium cyanoborohydride ($NaCNBH_3$), with pH adjusted to 4–5 with glacial AcOH. This reaction was carried out in MeOH under inert atmosphere, affording the β-amino ester (**20**) (Scheme 1). Next, the hydrazide intermediate (**21**) was synthetized by the treating of β-amino ester (**20**) with excess of hydrazine hydrate in ethanol under reflux.[30] This reaction led to the desired hydrazide (**21**) in 90% of yield (Scheme 1). The racemic β-aminohydrazide (**21**), obtained in five linear steps in 15% of overall yield, was outlined as the key intermediate for

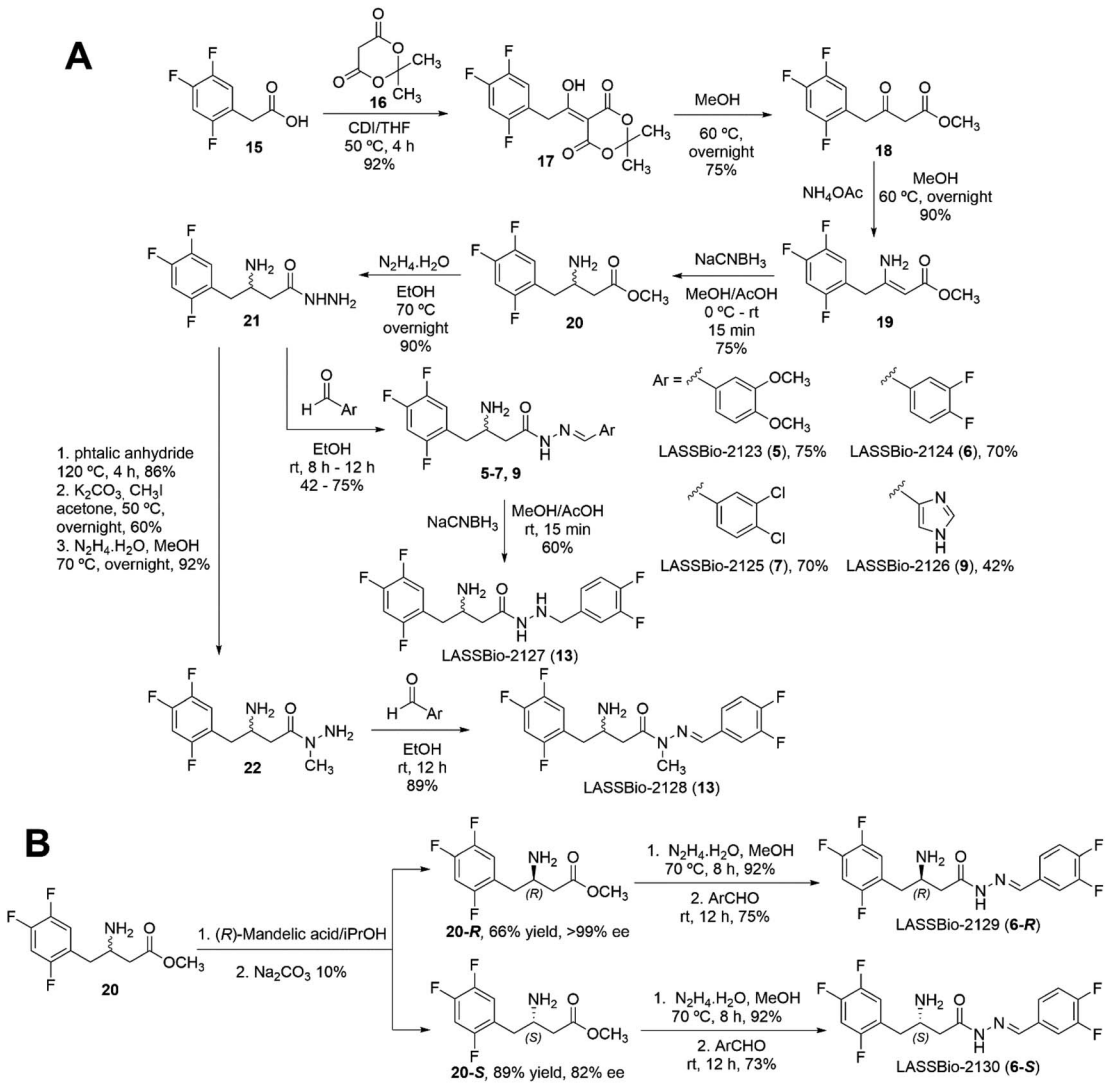

Scheme 1 (A) Synthesis of compounds (**5**–**7**), (**9**), (**13**–**14**) as racemic mixtures. (B) Methodology for the chiral resolution of β-aminoester (**20**) and its application in the synthesis of the target compounds (**6**-*R*) and (**6**-*S*).

the synthesis of target β-amino-*N*-acylhydrazone derivatives, designed as new DPP-4 inhibitors. With this intermediate in hand, we were able to obtain target compounds (**5**) (LASSBio-2123), (**6**) (LASSBio-2124), (**7**) (LASSBio-2125), and (**9**) (LASSBio-2126) by condensation reaction between the β-aminohydrazide intermediate (**21**) and the corresponding aldehydes dissolved in ethanol, at room temperature (Scheme 1).

Although the synthesised β-amino-*N*-acylhydrazones have showed a high degree of purity as assessed by high performance liquid chromatography (HPLC), signal duplication was observed in the ^{1}H and ^{13}C NMR spectra (ESI Table S5†). After a combination of different dynamic NMR and molecular modelling studies we proposed that the β-amino-*N*-acylhydrazones might exist in solution as a mixture of s-*cis* and s-*trans* conformers (Fig. 6). It is interesting to note that a similar conformational behaviour has been reported for some *N*-acylhydrazones by Lopes and colleagues.[31–34]

Regarding the geometry of the imine double bond, several pieces of evidence led us to propose an *E* configuration, firstly because this is the energetically favoured isomer,[31–34] and secondly because the chemical shift of the imine hydrogen at δ_H 8.15 in the NMR spectra performed at 90 °C is expected for this

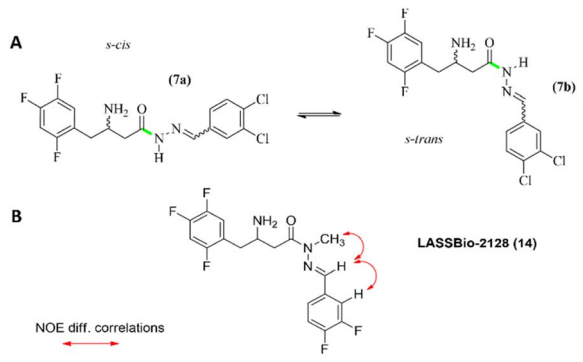

Fig. 6 (A) Conformers s-*cis* and s-*trans* of compound (**7**). (B) NOE correlations found for compound (**14**).

geometry, compared to the chemical shift for a *Z* configuration, which is expected at $\delta_H \approx 7.00$.[31,32] The *E*-geometry of the imine double was later confirmed by NOE studies on the target compound LASSBio-2128 (**14**), the direct analogue of LASSBio-2144 (**6**) (ESI Fig. S9†), as it will be described later.

The hydrazide target compound (**13**), designed as a non-conformationally restricted analogue of LASSBio-2124 (**6**), was synthesised from compound (**6**) by exploring the reduction of the imine double bond, using sodium cyanoborohydride in acid medium (Scheme 1).

The strategy used to obtain compound (**14**) (LASSBio-2128), the *N*-methyl analogue of LASSBio-2124 (**6**), was based on the protection of the two primary amine groups of the β-amine hydrazide (**21**) with phthalic anhydride, followed by methylation of the phthalimide intermediate product, its deprotection and subsequent condensation of the *N*-methyl-hydrazide with 3,4-diflurobenzaldehyde (Scheme 1). The desired LASSBio-2128 (**14**) was obtained in nine linear steps, in 15% of overall yield.

It is worth mentioning that no signal duplication was observed in the NMR spectra for LASSBio-2128 (**14**), which shows a different pattern when compared to the non-methylated β-amino-*N*-acylhydrazone (*i.e.*, LASSBio-2124, **6**). This fact can be explained considering that the *N*-methylation of the amide nitrogen of the β-amino-*N*-acylhydrazone scaffold causes a conformational restriction of the amide bond, preventing its rotation. Consequently, it reduces the existence of conformers and abolishes the duplication of the signals in the NMR spectra. These results also corroborate with the hypothesis of the existence of amide s-*cis*/s-*trans* conformers, which was previously mentioned in an attempt to explain the duplication of signals in the NMR spectra of LASSBio-2123 to LASSBio-2126 (**5–7**, **9**).

Furthermore, to confirm the relative configuration of LASSBio-2128 (**14**), NOE_{diff} experiments were performed. As depicted in Fig. S9 (ESI),† the experiments have revealed the spatial correlation between the irradiated hydrogens of the methyl group with the hydrogen of the imine function. These data allowed to confirm an *E* configuration of the imine double bond, as previously proposed, through the analysis of the chemical shifts of the amide and imine hydrogens of β-amino-*N*-acylhydrazone derivatives.

The second part of the synthetic plan was based on efforts to implement a synthetic methodology to separately obtain both *S* and *R*-enantiomers of the selected β-amino-*N*-acylhydrazone derivatives. We decided to explore the chiral resolution of the β-amino ester intermediate (**20**), followed by the reactions of hydrazinolysis and condensation with the selected aldehydes (Scheme 1B). We started with the formation of diastereomeric salts by treating the (***R***,***S***)-β-amino ester (**20**) with (*R*)-mandelic acid in isopropanol to furnish the mixture of the diastereoisomers, which were separated and purified by recrystallization. Separate treatment with Na_2CO_3 10% solution afforded the free amine (**20-*R***) with an enantiomeric excess greater than 99% and the amine (**20-*S***) with 82% of enantiomeric excess (ESI Section 4†).

It should be noted that an absolute stereochemistry of ***R*** was assigned to the intermediate (**20-*R***) (HPLC retention time: 28.7 min), and consequently ***S*** for the intermediate (**20-*S***) (HPLC retention time: 23.4 min). A detailed explanation of the determination of the absolute stereochemistry can be found in the ESI (Section 4.2).†

Once accomplished the resolution and determination of the absolute stereochemistry of the β-amino esters (**20-*R***) and (**20-*S***), the next step was the synthesis of the hydrazides (**21-*R***) and (**21-*S***), which was carried out by hydrazinolysis of the corresponding intermediates (**20-*R*** and **20-*S***) (Scheme 1). Finally, each of the enantiopure hydrazides (**21-*R*** and **21-*S***) were reacted with 3,4-difluorobenzaldehyde to give the target compounds LASSBio-2129 (**6-*R***) and LASSBio-2130 (**6-*R***).

With all the target compounds in hand, we decided to evaluate their key physicochemical properties, such as aqueous solubility, pK_a, and chemical stability.

Psychochemical properties assessment

Aqueous solubility at physiological pH (7.4) was measured by spectrophotometric assay for the target compounds LASSBio-2123 (**5**), LASSBio-2124 (**6**), LASSBio-2125 (**7**) and LASSBio-2126 (**9**) (ESI Section 5†). As shown in Table 2, all compounds exhibited aqueous solubility values greater than 24 mg mL^{-1} (≥66 μM). The high aqueous solubility of the free amines (**5–7**, **9**) (LASSBio-2123–LASSBio-2125), even considering the lipophilic properties of the aromatic subunit linked to the imine moiety, was attributed to the presence of the primary amine and its pK_a value, which should contribute to the ionization of the molecules at pH = 7.4. To confirm that, the experimental determination of dissociation constants of compounds LASSBio-2123 to LASSBio-2126 (**5–7**, **9**) was recognised as an important goal.

The dissociation constant, usually expressed as negative the logarithm (pK_a), indicates the degree of ionisation of acidic/basic compounds and is an important parameter influencing physicochemical properties such as lipophilicity, solubility, and permeability. In addition, the pK_a value is useful to assess the pharmacodynamic behaviour in the biophase of a given drug with ionisable groups. Thus, considering the presence of a β-amino group in the structure of our target compounds, and taking into account the pharmacophoric nature of this group, which makes key interactions with Glu205/206 in the active site of DPP-4,[26] the experimental dissociation constant values for compounds **5–7** and **9** was determined (ESI Section 6†). The experimental pK_a values for the target β-amino-*N*-acylhydrazone range from 7.51 to 8.05, indicating that at physiologic pH (7.4) compounds **5–7** and **9** exist in a mixture of dissociated and non-dissociated forms (probably with percentages close to the 50–

Table 2 Aqueous solubility values of compounds LASSBio-2123 to LASSBio-2126 (**5–7**, **9**)

Compound	Score value	R^2
LASSBio-2123 (**5**)	51.5 (105)	0.9999
LASSBio-2124 (**6**)	24.6 (66)	0.9999
LASSBio-2125 (**7**)	33.2 (82.4)	0.9999
LASSBio-2126 (**9**)	>48.8 (>150.1)	0.9954

60%), with the equilibrium tending towards the dissociated form. These data may explain the high aqueous solubility of these compounds and suggest that, as with sitagliptin (**1**), an ionic bridge-type interaction may be involved in the recognition of the β-amino group with the Glu residues in the active site of DPP-4. For compound LASSBio-2126 (**8**), the pK_a value of 4.43 indicates that the imidazole subunit is fully protonated at pH 7.4, which would explain its higher water solubility.

Finally, we considered studying the chemical stability of compounds (**5–7**, **9**) in an aqueous media with a pH system that could mimic the pH of the enzymatic test (pH 7.4) (ESI Section 7†), with the aim of verifying that these compounds maintain their physical and chemical properties unchanged to reach its target. In addition, we extended our chemical stability study to pH = 2.0 to see how these compounds behave in the acidic conditions of the stomach. The results indicated that in the neutral medium (pH 7.4), which mimics pH environment of the test, all the compounds were stable during the time analysed from 0 to 240 min, with less than 10% of degradation (Fig. 7). However, in acidic buffer (mimicking gastric pH) the compounds showed a degree of instability. LASSBio-2123 (**5**) and LASSBio-2124 (**6**) were degraded by about 20% in the first 30 min, increasing to 30% degradation from 60 min to the end of the experiments (after 240 min). LASSBio-2123 (**5**) showed slower degradation kinetics, with 30% of decomposition at 120 min and 50% of recovery after 240 min. Taken together, we have observed a lower stability of the target compounds in PBS pH = 2.0 compared to pH = 7.4. However, the instability was time dependent and did not exceed 30% in the first 2 hours.

These results indicate that our target compounds have adequate aqueous solubility and chemical stability under the test conditions. Additionally, a pK_a values of 7.7–8.05 led us to propose that these compounds could be protonated at the primary amine in the biophase. This is important considering that Glu266/265 are key pharmacophoric points capable of making ionic interactions with the primary amine of the tested compounds.

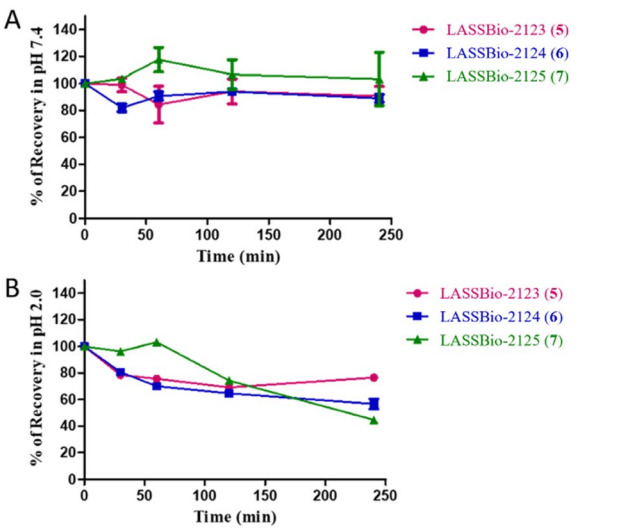

Fig. 7 Chemical stability of LASSBio-2123 (**5**), LASSBio-2124 (**6**) and LASSBio-2125 (**7**) (A) results at pH = 7.4. (B) Results at pH = 2.0. The experiments were conducted in triplicate, and the values shown represent the average of the experiments.

In vitro evaluation

After the synthesis and determination of key physicochemical parameters (solubility, pK_a and chemical stability) compounds **5** (LASSBio-2123), **6** (LASSBio-2124), **7** (LASSBio-2125), **9** (LASSBio-2126), **13** (LASSBio-2127), **14** LASSBio-2128, **6-*R*** (LASSBio-2129) and **6-*S*** (LASSBio-2130) were evaluated for their inhibition profile against human recombinant DPP-4 enzyme (Table 3).‡

We started the biological evaluation by validating the DPP-4 assay kit with (*R*)-sitagliptin (**1**).§ (*R*)-sitagliptin (**1**) showed inhibitory activity with an IC_{50} of 92 nM. This value was considered comparable to that reported in the literature (IC_{50} = 19 nM).[26] The difference was expected since the conditions of the literature's experiment (buffers and equipment) were not the same as those used in this DPP-4 assay. However, considering that both values (IC_{50} = 92 nM *vs.* IC_{50} = 19 nM) are in the same order of magnitude, we have considered the kit satisfactorily validated.

Next, we used the DPP-4 kit to investigate the concentration–response relationship and determine the IC_{50} values of compounds previously mentioned. As expected, LASSBio-1773 (**2**) was inactive. On the other hand, the new hybrid compounds LASSBio-2123 (**5**), LASSBio-2124 (**6**), LASSBio-2125 (**7**), LASSBio-2126 (**9**) showed activity in the same range of magnitude (IC_{50} = 10 to 74 μM), with LASSBio-2124 (**6**) being

Table 3 Potency (IC_{50} values) of LASSBio-2123 to LASSBio-2130 (**5–7**, **13**, **14**, **6-*R***, **6-*S***), LASSBio-1773 (**2**) and Sitagliptin (**1-*R***) against human recombinant DPP-4

Compound	Inhibition of DPP-4 IC_{50} (μM)[a]	R^2
(*R*)-Sitagliptin (**1-R**)	0.092	0.9991
LASSBio-1773 (**2**)	N.A.[b]	—
LASSBio-2123 (**5**)	34.3	0.9964
LASSBio-2124 (**6**)	10.6	0.9835
LASSBio-2125 (**7**)	30.8	0.9972
LASSBio-2126 (**9**)	24.0	0.9768
LASSBio-2127 (**13**)	2.93	0.9911
LASSBio-2128 (**14**)	74.67	0.9184
LASSBio-2129 (**6-R**)	5.08	0.9994
LASSBio-2130 (**6-S**)	44.74	0.9970

[a] The IC_{50} values displayed are the mean of three experiments in μM. [b] N.A. = no active.

‡ For the evaluation of the inhibitory activity of the compounds designed as DPP-4 inhibitors, we have acquired the DPP-4 inhibitor screening assay kit from cayman chemicals. The assay is based on a fluorometric test for screening and to establish the concentration–response curve of potential DPP-4-inhibitors (Cayman Chemicals, 2108).

§ We tested the (*R*)-sitagliptin (7) (free base) in concentrations ranging from 0.001 to 10 μM, to establish the half maximal inhibitory concentration (IC_{50}), and then compare the calculated IC_{50} value with that previous described in the literature.

most potent (Table 3). This result is consistent with the docking study (described above), which showed both *R* and *S* enantiomers of LASSBio-2124 (**6**) with higher score values (Table 1).

To analyse the effect of the stereochemistry of the β-amino group in the DPP-4 inhibition profile, docking studies projected the *R*-enantiomer of LASSBio-2124 (**6**) as being able to reproduce the interactions of (*R*)-sitagliptin in the active site of DPP-4. The comparison of LASSBio-2124 (racemate), LASSBio-2129 (*R*-isomer), LASSBio-2130 (*S*-isomer) is shown in Table 3. LASSBio-2129 (**6-*R***) showed a potency of 5.08 μM, while its antipode, LASSBio-2130 (**6-*S***), showed an IC_{50} = 44,74 μM. An almost nine-fold difference in the comparative potency of these compounds suggests that the *R*-enantiomer (LASSBio-2129, **6-*R***) is the eutomer, and the *S*-enantiomer (LASSBio-2130, **6-*S***) is the distomer (eudysmic ratio (ER): 8.8), whereas the ER described in literature for sitagliptin (**1**) is 22. The difference in potency of the enantiomers LASSBio-2129 (**6-*R***) and LASSBio-2130 (**6-*S***) was anticipated by docking studies, as previously discussed in the molecular modelling section. Surprisingly, the pharmacological results also demonstrated that there was no satisfactory gain in potency when we compared the inhibitory profile of the racemic mixture, LASSBio-2124 (**6**), with the *R*-eutomer, LASSBio-2129 (**6-*R***).

With regard to the geometry of the imine double bond, as suggested by molecular modelling studies, the β-amino-*N*-acylhydrazones with an *E*-geometry LASSBio-2123 (**5**), LASSBio-2124 (**6**), LASSBio-2125 (**7**) and LASSBio-2126 (**9**), tested as a racemic mixture, were able to inhibit the DPP-4 enzyme with IC_{50} values of 34.3, 10.6, 30.8 and 24.0 μM, respectively. These data clearly indicate that although the target compounds were active against human DPP-4, they showed lower potency when compared to (*R*)-sitagliptin (Table 3).

On the other hand, changes in the D-subunit did not result in a significant gain in potency and considering that no statistical difference was observed for the potency of compounds LASSBio-2123 (**5**), LASSBio-2125 (**7**) and LASSBio-2126 (**9**) (Table 3), we can assume that the stereoelectronic effects of the substituents linked to the imine subunit had little contribution to the inhibition of DPP-4. This assumption contradicts the docking results, discussed in the molecular modelling section. However, another important point to consider about the activity of these β-amino-*N*-acylhydrazones, is related to the duplicated signals obtained in the NMR spectra of the β-amino-*N*-acylhydrazones synthesised for this study. This behaviour was attributed to a mixture of two predominant conformations, s-*cis* and s-*trans*, even in polar solvents such as DMSO. This raises the possibility that these compounds, in the biophase, could be present in two different conformations with different affinities for DPP-4. In this respect, it is interesting to note that the s-*trans* conformation (Fig. 6B) proposed for LASSBio-2125 (**7**) resemble that projected for LASSBio-2128 (**14**) (Fig. 6B), which is considered inactive in the DPP-4 assay. Conformationally restricted analogues will be required to address this issue and should be included in new optimization campaigns.

The increase in conformational freedom obtained through by reducing of the imine double bond, has resulted in a more potent compound (IC_{50} = 2.93 μM) than LASSBio-2124 (**6**) (IC_{50} = 10.6 μM) and its enantiomers LASSBio-2129 (**6-*R***) and LASSBio-2130 (**6-*R***). The *N*-methyl analogue LASSBio-2128 (**14**) induced a strong decrease in the DPP-4 inhibition (IC_{50} = 74.8 μM). These results are consistent with the predicted activity suggested by the docking approach (see molecular modelling section).

Based on the described pharmacological results and considering the structural variables proposed at the beginning of the project, we have proposed a preliminary structure–activity relationship (Fig. 8). In summary, the 2,4,5-trifluorophenyl moiety has been highlighted as a relevant pharmacophoric point capable of making hydrophobic interactions, probably involving Phe357 (S2-pocket) or amino acid residues at the S1-pocket. The stereochemistry of the β-amino group was confirmed as important for the inhibitor potency, *e.g.*, LASSBio-2124 (**6**) has displayed an eudysmic ratio of 8.81, favouring the *R* configuration. Alkylation at the sp^3 nitrogen of the β-amino-*N*-acylhydrazones core was detrimental to activity. The conformational freedom introduced by the reduction of the imine double bond was favourable for DPP-4 inhibition. Substitution at the imine subunit did not play an important role in the inhibitory potency.

Having confirmed the ability of the designed target compounds to inhibit DDP4, the next challenge was to investigate whether such an inhibitory action would indeed imply an anti-diabetic effect *in vivo*. Therefore, we have selected LASSBio-2124 (**6**) to start the *in vivo* analysis. The criteria for this selection were because LASSBio-2124 (**6**), even in the racemic form, has shown a comparable potency to its *R*-enantiomer LASSBio-2129 (**6-*R***). Moreover, considering the experimental methodologies developed in this work, the racemic approach has proven to be more scalable, when compared to the resolution of the β-amino ester intermediate, followed by the synthesis of the pure enantiomer.

Two grams of LASSBio-2124 (**6**) were synthesised and tested in *in vivo* assays *via* oral administration, using a murine model of T2DM induced by a combination of high fat diet and streptozotocin. As demonstrated by Alves and coworkers, like (*R*)-sitagliptin, LASSBio-2124 (**6**) showed antihyperglycemic effects and improved cardiac and renal dysfunction, which are commonly observed disturbances in T2DM associated with metabolic syndrome.[35]

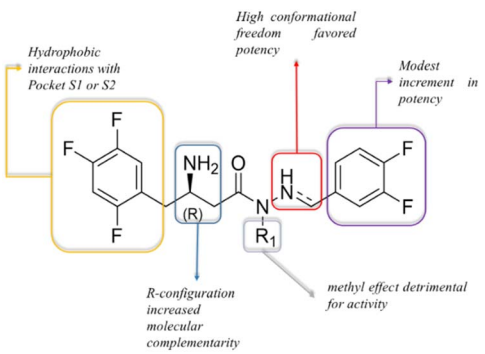

Fig. 8 Preliminary structure–activity relationships for LASSBio-2123 to LASSBio-2130 (**5–7**, **9**, **13**, **14**, **6-*R***, **6-*S***) as DPP-4 inhibitors.

Conclusions

In conclusion, a new kind of DPP-4 inhibitors were designed bearing a new β-amino-*N*-acylhydrazone framework, obtained by applying molecular hybridization between sitagliptin (**1**) and LASSBio-1773 (**2**) prototype. We evaluated five key variables of the β-amino-*N*-acylhydrazone core and their impact on DPP-4 inhibition. The stereochemistry of the β-amino group was important for activity, as well as the *E* geometry of the imine doubled bond, but the substituent on this region had little impact on potency and could be explored for optimization. On the other hand, an increase in conformational freedom obtained by reduction of the imine double bond, had a positive effect, resulting in LASSBio-2127 (**13**), with IC_{50} = 2.9 μM. Finally, the conformational change induced by the introduction of the *N*-methyl group had a detrimental effect on DPP-4 inhibition, as illustrated by LASSBio-2128 (**14**) (IC_{50} = 74.7 μM). In addition, these studies led us to identify LASSBio-2124 (**6**) as an authentic lead with good physicochemical properties, good DPP4 inhibition potency and *in vivo* antidiabetic activity, which can be synthesized in its racemic or pure enantiomeric form and used in future lead-optimization campaigns.

Conflicts of interest

There are no conflicts to declare.

Acknowledgements

This work was supported by Conselho Nacional de Desenvolvimento Científico e Tecnológico (CNPq), Coordenação de Aperfeiçoamento de Pessoal de Nível Superior (CAPES), Fundação Carlos Chagas Filho de Amparo à Pesquisa do Estado do Rio de Janeiro (FAPERJ), Instituto Nacional de Ciência e Tecnologia de Fármacos e Medicamentos (INCT-INOFAR).

Notes and references

1 L. Emami, Z. Faghih, A. Sakhteman, Z. Rezaei, Z. Faghih, F. Salehi and S. Khabnadideh, *New J. Chem.*, 2020, **44**, 19515–19531.
2 E. E. Mulvihill and D. J. Drucker, *Endocr. Rev.*, 2014, **35**, 992–1019.
3 J. Fremaux, C. Venin, L. Mauran, R. Zimmer, F. Koensgen, D. Rognan, S. Bitsi, M. A. Lucey, B. Jones, A. Tomas, G. Guichard and S. R. Goudreau, *Chem. Sci.*, 2019, **10**, 9872–9879.
4 C. F. Deacon, *Nat. Rev. Endocrinol.*, 2020, **16**, 642–653.
5 L. Juillerat-Jeanneret, *J. Med. Chem.*, 2014, **57**, 2197–2212.
6 S. Costes, G. Bertrand and M. A. Ravier, *Int. J. Mol. Sci.*, 2021, **22**, 5303.
7 D. Kannenkeril, A. Bosch, J. Harazny, M. Karg, S. Jung, C. Ott and R. E. Schmieder, *Cardiovasc. Diabetol.*, 2018, **17**, 128.
8 B. D. Patel and M. D. Ghate, *Eur. J. Med. Chem.*, 2014, **74**, 574–605.
9 L. M. Lima, G. Zapata-Sudo, I. K. da Costa Nunes, J. Segundo Chaves de Araujo, J. da Silva, M. Manhães Trachez, T. Fernandes da Silva, F. P. da Costa, R. Sudo and E. Barreiro, *Drug Des., Dev. Ther.*, 2016, **10**, 2869–2879.
10 G. Zapata-Sudo, L. M. Lima, S. L. Pereira, M. M. Trachez, F. P. da Costa, B. J. Souza, C. E. S. Monteiro, N. C. Romeiro, E. D. D'Andrea, R. T. Sudo and E. J. Barreiro, *Curr. Top. Med. Chem.*, 2012, **12**, 2037–2048.
11 L. M. Lima, M. M. Trachez, J. S. C. Araújo, J. S. Silva, D. N. Amaral, R. T. Sudo, E. J. Barreiro and G. Zapata-Sudo, *J. Diabetes Metab.*, 2014, **5**, 392.
12 S. Kumar, A. Mittal and A. Mittal, *Bioorg. Med. Chem.*, 2021, **46**, 116354.
13 K. Tomovic, B. S. Ilic and A. Smelcerovic, *J. Med. Chem.*, 2021, **64**, 9639–9648.
14 J. Zhong, A. Maiseyeu, S. N. Davis and S. Rajagopalan, *Circ. Res.*, 2015, **116**, 1491–1504.
15 Q. Gong, S. Rajagopalan and J. Zhong, *Int. J. Cardiol.*, 2015, **197**, 170–179.
16 H. Liu, L. Guo, J. Xing, P. Li, H. Sang, X. Hu, Y. Du, L. Zhao, R. Song and H. Gu, *Eur. J. Pharmacol.*, 2020, **875**, 173037.
17 E. Angelopoulou and C. Piperi, *Ann. Transl. Med.*, 2018, **6**, 255.
18 Y. Chen, J. Zhang, B. Zhang and C.-X. Gong, *Curr. Top. Med. Chem.*, 2015, **16**, 485–492.
19 N. S. S. Chalichem, P. S. S. Sai Kiran and D. Basavan, *J. Drug Targeting*, 2018, **26**, 670–675.
20 Y. Ohyagi, K. Miyoshi and N. Nakamura, Therapeutic Strategies for Alzheimer's Disease in the View of Diabetes Mellitus, in *Diabetes Mellitus, Advances in Experimental Medicine and Biology*, ed. Y. Nakabeppu and T. Ninomiya, Springer, Singapore, 2019, vol. 1128, pp. 227–248.
21 R. Strollo and P. Pozzilli, *Diabetes/Metab. Res. Rev.*, 2020, **36**(8), e3330.
22 S. B. Solerte, A. Di Sabatino, M. Galli and P. Fiorina, *Acta Diabetol.*, 2020, **57**, 779–783.
23 L. M. Lima and E. J. Barreiro, in *Comprehensive Medicinal Chemistry III*, Elsevier, New York, 2017, vol. 1–8, pp. 186–210.
24 L. Lima and E. Barreiro, *Curr. Med. Chem.*, 2005, **12**, 23–49.
25 S. Thota, D. A. Rodrigues, P. de S. M. Pinheiro, L. M. Lima, C. A. M. Fraga and E. J. Barreiro, *Bioorg. Med. Chem. Lett.*, 2018, **28**, 2797–2806.
26 D. Kim, L. Wang, M. Beconi, G. J. Eiermann, M. H. Fisher, H. He, G. J. Hickey, J. E. Kowalchick, B. Leiting, K. Lyons, F. Marsilio, M. E. McCann, R. A. Patel, A. Petrov, G. Scapin, S. B. Patel, R. S. Roy, J. K. Wu, M. J. Wyvratt, B. B. Zhang, L. Zhu, N. A. Thornberry and A. E. Weber, *J. Med. Chem.*, 2005, **48**, 141–151.
27 E. J. Barreiro, A. E. Kümmerle and C. A. M. Fraga, *Chem. Rev.*, 2011, **111**, 5215–5246.
28 M. Eckhardt, E. Langkopf, M. Mark, M. Tadayyon, L. Thomas, H. Nar, W. Pfrengle, B. Guth, R. Lotz, P. Sieger, H. Fuchs and F. Himmelsbach, *J. Med. Chem.*, 2007, **50**, 6450–6453.
29 P. Sun, Y. Chen, and G. YU, Process for Preparing R-Beta-Amino Phenylbutyric Acid Derivatives, *US Pat.*, US2011/0130587 A1, 2011.
30 A. E. Kümmerle, M. Schmitt, S. V. S. Cardozo, C. Lugnier, P. Villa, A. B. Lopes, N. C. Romeiro, H. Justiniano,

M. A. Martins, C. A. M. Fraga, J.-J. Bourguignon and E. J. Barreiro, *J. Med. Chem.*, 2012, **55**, 7525–7545.

31 A. Lopes, E. Miguez, A. Kümmerle, V. Rumjanek, C. Fraga and E. Barreiro, *Molecules*, 2013, **18**, 11683–11704.

32 G. Palla, G. Predieri, P. Domiano, C. Vignali and W. Turner, *Tetrahedron*, 1986, **42**, 3649–3654.

33 P. Kumar, K. Kadyan, M. Duhan, J. Sindhu, V. Singh and B. S. Saharan, *Chem. Cent. J.*, 2017, **11**, 115.

34 T. F. Silva, W. Bispo Júnior, M. S. Alexandre-Moreira, F. N. Costa, C. Monteiro, F. Furlan Ferreira, R. C. R. Barroso, F. Noël, R. T. Sudo, G. Zapata-Sudo, L. M. Lima and E. Barreiro, *Molecules*, 2015, **20**, 3067–3088.

35 B. E. O. Alves, A. K. N. de Alencar, L. E. R. Gamba, M. M. Trachez, J. S. da Silva, J. S. C. Araújo, T. L. Montagnoli, L. V. P. Mendes, P. M. Pimentel-Coelho, V. do M. N. Cunha, R. Mendez-Otero, G. M. M. Oliveira, L. M. Lima, E. J. Barreiro, R. T. Sudo and G. Zapata-Sudo, *Pharmacol. Rep.*, 2019, **71**, 1190–1200.